WILEY-VCH

Recycling of Nanowire Percolation Network for Sustainable Wearable Electronics

Yuxuan Liu,[1] *Hongyu Wang,*[1] *Yong Zhu*[1,2,3*]

[1]Department of Mechanical and Aerospace Engineering, North Carolina State University, Raleigh, NC 27695, USA.

[2]Joint Department of Biomedical Engineering, North Carolina State University, Raleigh, NC 27695, USA; University of North Carolina at Chapel Hill, Chapel Hill, NC 27599, USA.

[3]Department of Materials Science and Engineering, North Carolina State University, Raleigh, NC 27695, USA.

[*] To whom correspondence should be addressed: Yong Zhu (yzhu7@ncsu.edu)

Keywords: Recycling; silver nanowire; sustainable electronics; wearable electronics

Abstract

There is an increasing demand for eco-friendly and sustainable electronics, where recycling of functional materials is the key. Wearable electronics have received much attention recently, however, their recycling has been challenging. Here we report a strategy to recycle silver nanowire (AgNW) percolation network to achieve sustainable wearable electronics. The effect of working solvent and ultrasonication time on the morphology and electrical properties of the recycled AgNW network is investigated. Using the selected working solvent with low surface tension (isopropanol) and optimal ultrasonication time (20 s), the AgNW network film can be recycled multiple times (4 times in this work) without significant morphology changes and performance degradation. A transient epidermal sensor patch using AgNW as electrodes and a water-soluble polymer substrate is fabricated and fully recycled. On-body test of the epidermal sensor patch fabricated by recycled AgNWs demonstrates a working example for the recycling concept of AgNWs. The recycling concept can be extended to other nanomaterials in the form of percolation network.

1. Introduction

More and more electronics are used in different facets of human life, yet their lifetime in use is showing a generally shortening trend (e.g., smartphones). As a result, two important challenges have emerged: i) a huge amount of waste from used electronics, posing hazardous threat to the environment [1-3] and ii) rapid consumption of scarce elements such as noble and rare-earth metals to manufacture electronic devices.[4] There is an increasing demand for eco-friendly and sustainable electronics, where the recycling of functional materials is the key.

Wearable electronics with desirable flexibility and stretchability have enabled a wide range of applications where electronic devices undergo large deformation and/or form intimate contact with curvilinear surfaces. [5-15] In the physically transient form of flexible and stretchable electronics, functional materials disintegrate and/or dissolve at the end of their lifetime in use. [16-19] This feature can be highly desirable for many applications ranging from implantable medical diagnostic and therapeutic devices to field deployable environmental sensors. For example, implantable devices are desirable to resorb in the body to avoid adverse long-term effects and environmental sensors could dissolve to eliminate the need for their retrieval. Both inorganic semiconductors (e.g., Si) and organic semiconductors have been used to fabricate transient electronics. While this "transient" feature is appealing, it does not address the two aforementioned challenges, at least directly, as the disintegrated or dissolved materials would still go to the environment without recycling.

Recycling all or even part of the functional materials would help address the challenges. This is unfortunately very challenging, if possible at all, for functional materials that are fabricated using the top-down approach (e.g., deposited at relatively high temperatures). Materials that are

fabricated by the bottom-up approach could be a viable alternative. As shown in **Figure 1**a, a composite containing functional materials in a dissolvable polymer matrix can be recycled by dissolving the polymer matrix and dispersing the functional materials; both the polymer and functional materials can be reused for fabricating new devices. Conductive nanocomposites have been reported by doping conductive nanoparticles in a polymer matrix, but with limited flexibility and low electrical conductivity. [20] Directly printed percolation network of nanomaterials could achieve much higher flexibility and conductivity, showing promise for high-performance wearable electronics.

In this work, we demonstrate this concept using silver nanowire (AgNW) percolation network as an example. AgNWs have been widely used as electrodes and conductors in many applications of flexible/stretchable electronics, [21-23] wearable devices, [24-27] and transparent electrodes. [28-32] Here, we present an effective and facile recycling procedure for drop-casted AgNW network film for sustainable flexible and stretchable electronics. Ultrasonication is used to separate the NW network. The effect of two important factors – working solvent and ultrasonication time – on the morphology and electrical properties of the recycled AgNW network is systematically studied. The best working solvent and optimal ultrasonication time are determined, which are used for recycling the same batch of AgNWs multiple times (e.g., 4 in our case) with still acceptable electrical properties. A transient epidermal sensor patch using AgNW as electrodes and a water-soluble polymer substrate is fabricated and fully recycled. On-body test of the epidermal sensor patch fabricated by recycled AgNWs demonstrates a working example for the recycling concept of AgNWs. Note that the AgNW network used in this work is as deposited, without any annealing.

The recycling concept can be extended to other nanomaterials in the form of percolation network such as nanoparticles, carbon nanotubes and 2D materials. [8, 33-35]

2. Results and Discussion

2.1 Effect of Solvent

Ultrasonication is widely used to deagglomerate and disperse nanomaterials in solvent.[36] Ultrasonication generates alternating low-pressure and high-pressure waves in liquids, leading to formation and rapid collapse of microbubbles. This process causes high-speed impinging liquid jets and strong hydrodynamic shear force, which can be used for deagglomeration of nanomaterials. However, it is much more challenging to re-disperse dried NW percolation network in solvent. For a dried NW network film, NWs are connected with each other by van der Waals forces at the junctions. To separate the dried NWs, diffusion of the solvent into the junctions is a prerequisite so that the hydrodynamic shear force can form at the NW junctions during ultrasonication. After separation of the NWs, stabilization of the NWs in solvent should also be addressed. A widely used stabilization strategy for AgNWs is coating a layer of polyvinylpyrrolidone (PVP) on NW surface, which leads to steric effects to maintain balance between the attractive and repulsive forces. [37-39] Therefore, two aspects need to be considered in order to choose the desirable working solvent to re-disperse the dried NW network by ultrasonication. First, a solvent with relatively low surface tension (γ) should be chosen so that the solvent molecules can diffuse into the NW junctions more easily. Second, the solvent should be PVP soluble to ensure the stabilization of the re-dispersed AgNWs in the solvent.

Several PVP-soluble solvents including alcohol (methanol (MeOH), ethanol (EtOH), isopropanol (IPA)), ethylene glycol (EG) and DI water were investigated as the working solvents. The ultrasonication time was 20 s for all the solvents. Figure 1b shows the schematic illustration of the recycling process of drop-casted AgNW percolation networks. Ultrasonication and centrifugation are two main steps in this process. More details of the recycling process can be found in Experimental Section. **Figures 2**a-d show the representative Scanning Electron Microscope (SEM) images of the original AgNW network and the recycled AgNW network using IPA, EG and DI water as the working solvents. It can be seen that the IPA recycled AgNW network shows similar morphology to the original. EG recycled AgNW network exhibits nonuniform distribution with discrete agglomerations, while DI water recycled AgNW network severely agglomerates. Precipitate residues can be observed at the bottom of the EG and DI water recycled AgNW solutions after ultrasonication.

Figures 2e-h show the Area Fraction (AF) distribution and the Gaussian fit of the original AgNW network and the recycled AgNW network using IPA, EG, and DI water as the working solvents. Note that all the original and recycled AgNW networks are formed by drop casting; in the case of recycled AgNWs, they go through the process of ultrasonication and centrifugation before drop casting. Average Area Fraction ($\overline{AF}$) is calculated in each case to characterize the loading density of the AgNW network film. The original AgNW network shows $\overline{AF}$ of 33.44%, while the IPA, EG, and DI water recycled AgNW networks show $\overline{AF}$ of 33.03%, 32.42%, and 32.46%, respectively. Recycling by different solvents results in similar $\overline{AF}$, however, the standard deviations of the area fraction (σ_{AF}) differ markedly. Narrow distribution with a small σ_{AF} indicates uniform network, while wide distribution with a large σ_{AF} represents nonuniform network with

randomly distributed agglomerations and low-density areas. Compared with the original AgNW network with σ_{AF} of 4.97%, the IPA, EG, and DI water recycled AgNW networks show σ_{AF} of 7.22%, 9.21%, and 26.49%, respectively, indicating increasing nonuniformity of the networks. These results are consistent with the SEM images (Figures 2a-d). Thus, σ_{AF} can be used to characterize the agglomeration level (or uniformity) of the network in the following analysis.

Figure 2i depicts the sheet resistance change (left axis, ΔR = the sheet resistance change and R_0 = the sheet resistance of the original AgNW network) and σ_{AF} (right axis) of the original AgNW network and the recycled AgNW networks using IPA, EtOH, MeOH, EG, and DI water as the working solvents. The inset table lists the surface tension γ in air at 20 ℃ of these solvents. The γ values of alcohol (IPA, EtOH, and MeOH) are similar. EG has a higher γ of 48 mN/m, and DI water has the highest γ of 72 mN/m among all. [40] The contact angle measurements of IPA, EG, and DI water on AgNW network film are shown in **Figure S1**. As expected, the solvents with higher γ exhibit larger contact angles. Compared to the original AgNW network with a sheet resistance of 24.5 Ω/sq, the IPA, EtOH, and MeOH recycled AgNW networks exhibit slightly increasing sheet resistances, respectively. The EG and DI water recycled networks exhibit much higher sheet resistance change by 10-fold and 160-fold, respectively. σ_{AF} of different recycled networks shows a similar trend to the sheet resistance, indicating that the higher sheet resistance is caused by the nonuniformity in the AgNW network (i.e., higher agglomeration level). IPA was used as the working solvent in the rest of this work.

We have shown that both the sheet resistance and σ_{AF} increase with the increasing γ. Although alcohol, EG, and water used here are able to wet the AgNW network macroscopically (with small

contact angles on the network film, 15.6°, 48.6°, and 66.3°, respectively, as shown in Figure S1), it is challenging for the solvents with high surface tension to diffuse into the minuscule wire-wire gaps in the junctions, even with ultrasonication. The schematic diagrams of wetting the AgNW junctions are shown in Figure 2j. High γ solvent preferentially accumulates in the pores formed in the network without wetting the wire-wire gaps, while low γ solvent can fill in both the pores of the network and the wire-wire gaps. Without sufficient wetting of the wire-wire gaps at the junctions, a AgNW network cannot be separated because of the absence of the shear force generated by ultrasonication at the junctions. The unseparated AgNWs are suspended in solvent, which is the main source of the agglomeration, leading to the increased sheet resistance.

2.2 Effect of Ultrasonication Time

Now that ultrasonication demonstrates feasibility to re-disperse a dried AgNW network in selected solvents, we need to optimize the ultrasonication time. On one hand, the time should be sufficiently long to ensure separation of the NWs. On the other hand, the time should be short as ultrasonication-induced scission can break NWs as well. [41] According to the percolation theory, the NW length can strongly affect the electrical and optical properties of a AgNW network. [42-44] For the same network density, the longer the NWs, the higher the electric conductivity.

To determine the optimal ultrasonication time, AgNW network films with mass loading density of 20 μg/cm^2 were recycled in IPA with different ultrasonication time ranging from 5 to 60 s. Note that for all experiments in this work, the ultrasonication power at 100 W was used. The morphology of the original and recycled AgNW networks is shown in **Figures 3**a-d and **Figures S2**a-b. When the ultrasonication time is relatively short (i.e., less than 20 s), the AgNW networks are not

separated properly, leading to agglomerations in the recycled NWs, as shown in **Figure S2**a and b and represented by relatively large σ_{AF} (Figure S2c and d). The length distribution and the average length $\bar{L}$ do not change apparently (Figure 3i). This is because the limited energy from ultrasonication is used mainly to separate the AgNW network rather than breaking the isolated AgNWs. With increasing ultrasonication time over 20 s, no agglomerations remain in the recycled NWs, as represented by a nearly constant σ_{AF} (Figure S2e-g). But the NWs could be shortened compared with the original ones (Figures 3a-d). Quantitatively $\bar{L}$ decreases markedly with the increasing ultrasonication time, as shown in Figure 3i. After the backbone of the network is dispersed, scission of AgNWs ensues. It is found that $\bar{L}$ follows a power-law relation with the exponential factor of -0.6, consistent with reported studies on ultrasonic scission of 1D nanomaterials. [45, 46]

$\overline{AF}$ as a function of the ultrasonication time is shown in Figure S2h, where the error bar represents σ_{AF}. It can be seen that $\overline{AF}$ is nearly independent of the ultrasonication time. Note that in this experiment almost all the AgNWs are recycled in one cycle of the ultrasonication-centrifugation process, so the density of the network remains unchanged before and after the recycling. In the subsequent experiments for multiple recycling, severely shortened NWs will be removed in the centrifugation step.

Figure 3j shows the sheet resistance of the recycled AgNW network as a function of the ultrasonication time. Compared with the original AgNW network, the sheet resistance decreases with the increasing ultrasonication time when the time is less than 20 s but then increases with the increasing time. The decrease of the sheet resistance within 20 s is due to the decreasing level of

NW agglomeration. Over 20 s, the increasing sheet resistance can be attributed to the shortening of AgNWs. Therefore, 20 s is the optimal ultrasonication time in our work with the ultrasonication power of 100 W.

2.3 Multiple Recycling

Recycling functional materials for multiple times would be ideal for ecofriendly and low-cost manufacturing. The challenge is, however, to maintain the device performance to a reasonable extent. We evaluated the feasibility of multiple recycling of AgNWs, where the same ultrasonication-centrifugation recycling process was repeated multiple times without modification. **Figure 4** and **Figure S3** show the morphology and electrical performance of the AgNW network after different numbers of recycling. As shown in Figure 4a-d and Figure S3, the recycled AgNW network show only slight changes in morphology within the first four times of recycling. After recycling the same batch of AgNWs for 7 times, the nonuniformity of the NW network becomes evident. The length distributions with corresponding Gaussian fits are shown in Figure 4e-h. It can be seen that $\bar{L}$ of the recycled AgNWs reduces with the increasing number of recycling due to the scission caused by ultrasonication in each recycling, from the original 35.57 μm to 22.05 μm after the 7th recycling (Figure 4m). The AF distributions with corresponding Gaussian fits are shown in Figure 4i-f. $\overline{AF}$ reduces from the original 32.6% to 26.8% after the 7th recycling as a result of the AgNW loss during the multiple centrifugation steps. Also the distributions become wider with larger σ_{AF} with the increasing number of recycling. As shown in Figure 4m, $\overline{AF}$ is nearly unchanged for the 1st recycling. But the AgNW loss needs to be considered for multiple recycling, because repeated ultrasonication produces severely shortened NWs that are removed by centrifugation. The increase of σ_{AF} (error bar of the histogram in Figure 4m) indicates that the

recycled AgNW network becomes increasingly nonuniform with the increasing number of recycling. In addition to the insufficient separation of NWs, the nonuniformity in the NW network may be attributed to removal of PVP coating on the AgNW surface during the recycling. It has been shown that repeated centrifugation and dispersion can delaminate the PVP coating from AgNWs and result in agglomeration of AgNWs. [47, 48]

The sheet resistance change of the recycled AgNW network as a function of the recycling number is shown in Figure 4n. The sheet resistance increases by less than 100% within the first four times of recycling (shown in the inset), but increases dramatically from the 5th to the 7th recycling. Figure S3 shows optical images (with black background) and more SEM images of the originally drop-casted film and the ones after 1st, 4th and 7th recycling. The film remains uniform after the 1st recycling, but shows small visible clusters after the 4th recycling. The nonuniformity gets serious after the 7th recycling, with agglomeration and absence of NWs all over the film.

The ultrasonication and centrifugation processes could modify the surface status of NWs by removing the PVP capping layer, leading to the agglomeration. To quantify the removal of the PVP layer, zeta-potential values after different numbers of recycling processes were measured. Zeta potential characterizes the surface charging status of a particle suspended in a dispersion medium. The removal of PVP layer could cause the AgNW surface having less negative charge since PVP is a negatively charged surfactant, which would be manifested by a lower absolute zeta potential, as shown in Figure S4. It can be seen that with the increase of recycling number, the absolute zeta potential value decreases monotonously due to the removal of the PVP capping layer. The loss of the PVP layer is one of the main reasons that limits the recycling number.

Based on the discussions above, the increasing sheet resistance with the increasing number of recycling can be attributed to the following: 1) the decrease of $\bar{L}$ caused by scission effect of ultrasonication, 2) the decrease of $\overline{AF}$ due to AgNW loss, and 3) the increase of nonuniformity as a result of insufficient separation and removal of PVP coating. According to the percolation theory, the conductivity of a random percolation network depends on the loading density (i.e., $\overline{AF}$ in this work) and the average length of NWs $\bar{L}$, where the conductivity decreases with the decreasing density and $\bar{L}$. Agglomeration decreases the fraction of the current carrying backbone in the percolation network, which also causes decrease in the conductivity. As the electrical properties drop with each recycling, it is relevant to specify the acceptable criterion. If we take less than 100% increase in take the sheet resistance as acceptable, our recycling process can provide 4 times of recycling to the AgNW network film.

2.4 Recycling of AgNW based Transient Electronics

To demonstrate the application of the recycling strategy of NW percolation network for sustainable transient electronics, a thin sensor patch was fabricated including a temperature sensor and a hydration sensor (**Figures 5a)**. Following a previously reported fabrication process, [22, 29] AgNWs were encased in a PVA substrate. PVA was chosen because of its high solubility in water, which makes it an excellent candidate for transient and potentially recyclable electronics. Furthermore, PVA exhibit limited interactions with AgNWs in aqueous solution, [37] hence the AgNW surface will not be modified by PVA. The schematic illustration of recycling the transient sensor patch is shown in Figure 5a. Details on the fabrication of the sensor patch can be found in Experimental Section. The sensor patch can form conformal contact with the skin due to van der Waals

interactions (Figure 5b) and be peeled off without damaging the sensor patch or leaving residues on the skin (Figure 5c).

To recycle the entire sensor patch with both AgNWs and PVA, the recycling procedure was modified as following. The used sensor patch is firstly soaked in 100 mL DI water after being peeled off, as shown in Figure 5d. After soaked for 1 m, the electronics start to disintegrate including dissolution of the PVA substrate (Figure 5e). After soaked for 24 h, the AgNW electrodes are disintegrated into small pieces and precipitated to the bottom of the petri dish, while the PVA substrate is already dissolved in water (Figure 5f). Then the PVA aqueous solution is removed by centrifugation for further use, and the AgNW film pieces are collected and transferred to IPA solvent (Figure 5g). After following the same procedure described earlier, a homogeneous AgNW suspension as shown in Figure 5h is obtained, which can be drop casted again for device fabrication.

2.5 Demonstration of Sensor Applications

The aforementioned sensor patch fabricated by the recycled AgNWs was tested on body to demonstrate the epidermal application for real-time monitoring of human physiological parameters. **Figure 6**a shows the resistance change of the recycled temperature sensor when the temperature ranges from 20 to 60 °C in an incremental or decending manner. The sensor exhibits a stable and sensitive response to temperature change with excellent reversibility. Comparing with the original temperature sensor before the recycling (**Figure S5**), the recycled temperature sensor shows a slight decrease of temperature coefficent of resistance (TCR) from 2.99×10^{-3} $°C^{-1}$ (inset of Figure S4) to 2.88×10^{-3} $°C^{-1}$ (inset of Figure 6a). This may caused by the length decrease of the recycled

NWs. Figure 6b shows the real-time temperature data from an on-body test. The recycled temperature sensor was attached on the flexor side of the forearm. During the test, the subject went outdoor (ambient temperature ~ 30 ℃) and back to indoor (ambient temperature ~ 20 ℃) back and forth. The measured resistance change versus time shows a good agreement with the expected temperature change.

To evaluate the performance of the epidermal hydration sensor, the impedance change was recorded to characterize the hydration level of human skin. When the water content of the skin increases, the dielectric constant and the conductivity of the epidermis increase, leading to decrease of the impedance. [24, 49] After applying lotion to the skin to change the skin hydration level, the original and recycled sensors were attached to the skin to track the skin impedance in the following 30 m, as shown in Figure 6c and Figure S6a. The impedance values at 100 kHz before and after applying lotion were extracted (Figure 6d and Figure S6b). It can be seen that the skin impedance decreases significantly after applying lotion to the skin, manifesting the increasing hydration level of the skin. Then the impedance decreases gradually and recovers to the initial level in 30 m. The equivalent circuit model of the measuring system can be simplified as an RC circuit. [24, 49] The equivalent resistance and capacitance in the RC circuit of the original and recycled sensors are extracted from the impedance spectrum, as shown in Figure S6c and d. It can be seen that the equivalent resistance increases with time after applying the lotion, while the hydration level decreases. Compared to the original hydration sensor, the recycled sensor exhibits a slightly higher resistance, while showing the same trend. The equivalent capacitance decreases with the decrease of the hydration level, showing nearly the same results for the original and recycled sensors. These results show that the recycling process does not change the sensor performance significantly. The

epidermal temperature and hydration sensors fabricated using the recycled AgNWs demonstrate the potential applications of recycling NWs in sustainable transient electronics.

Briefly, the recycling of AgNW enabled wearable electronics consists of two steps: first, dissolving the polymer substrate with proper solvent; second, collecting and dispersing the AgNWs. Different substrate materials could be used. The only limitation comes from that the solvent dissolving the substrate should be compatible with the capping layer on the AgNW surface (i.e., PVP in this case), in other words, the solvent cannot damage the capping layer. Here we used another substrate material, thermoplastic polyurethane (TPU), to demonstrate the applicability of the recycling approach. The AgNW percolation network is embedded below the surface of a TPU film. [50] The recycling of a used AgNW/TPU film starts with soaking the film in dimethylformamide (DMF) solvent for 24 hours to dissolve TPU, as shown in Figure S7a and b. Then the AgNW segments are collected and transferred to an IPA solvent (Figure S7c). Following the same procedure described earlier, a homogeneous AgNW suspension, as shown in Figure S7d, is obtained and ready for further use. The original and recycled AgNWs are shown in Figure S7e and f, respectively. It can be seen that the AgNW network well maintains its uniform morphology after the recycling. In the future, we will explore a wide range of substrate materials by identifying suitable solvents that are compatible with the capping layer and/or researching new capping layers.

In this work, the recycling of the drop-casted NW networks was limited to the size of the glass slide used (2 cm by 2 cm). However, the recycling process is inherently scalable, e.g., by increasing the size and/or number of the substrate. The process parameters including solvent volume and ultrasonication time may need to be adjusted according to the amount of NWs recycled. For

transient electronics with a soluble substrate, the scalability can be improved by dissolving multiple used devices simultaneously in a substrate-soluble solvent (i.e., water for PVA substrate) and collecting the NWs after dissolution of the substrate. The following process of recycling the NWs is the same as that for a single device. Note that in this work, we used a relative low loading density of 20 μg/cm^2 in order to clearly observe the morphology of the AgNW network. With increasing loading density, the sheet resistance will decrease. A typical drop-casted AgNW percolation network had the sheet resistance ~0.2 Ω/sq. [22, 27] The thickness of the drop-casted AgNW network was reported to be from one to several μm, [22] hence, the conductivity can be over 10^4 S/m, much higher than that in the conductive composites with Ag nanoaparticles.[20]

3. Conclusion

This work presented an effective, reliable, and facile procedure for recycling drop-casted AgNW network for sustainable wearable electronics. The network morphology and electrical properties strongly depend on the working solvent used during the ultrasonication re-dispersion process. A PVP-soluble working solvent with relatively surface tension generally performs better. Out of the several working solvents studied, IPA was selected. An optimal ultrasonication time was found for the AgNW network film with a specific loading density and a constant ultrasonication power. AgNWs cannot be separated sufficiently when the ultrasonication time is short, but can be shorten severely if the time is excessive. Using the selected working solvent (IPA) and optimal ultrasonication time (20 s), the AgNW network film was recycled for multiple times without significant morphology changes and performance degradation. A transient epidermal sensor patch using AgNW as electrodes and a water-soluble PVA substrate was fabricated and fully recycled. The recycled sensor patch showed comparable on-body sensing performances to the original one.

This work demonstrated the concept of recycling AgNW network films for sustainable electronics. The recycling concept can be extended to other nanomaterials such as nanoparticles, carbon nanotubes, other types of NWs, and 2D materials, in the form of percolation network. While this work demonstrated a promising recycling approach for nanowires, at the present form the approach has limitations, leading to practically no more than 4 times of recycling. For the future work, we will investigate the fundamental aspects related to colloid stability throughout the recycling process to further improve the recycling efficacy. In addition, we will study the interactions between the AgNWs/surface capping agent, the substrate, and the dissolving solvent, such that more types of recyclable substrates can be used to achieve the complete recycling of electronic devices.

4. Experimental Section

Recycling of drop casted AgNWs: The original AgNW networks were fabricated by a simple drop-casting method. The AgNWs were synthesized by a modified polyol method. Glass slides with size of 2 cm by 2 cm were used as the substrate. A typical sample with a loading density of 20 μg/cm^2 was prepared by drop-casting 1 mL AgNW solution in ethanol (0.08 mg/mL) on the substrate and drying it in ambient air at 50 °C. Recycling of the dried AgNW network began with immersing the sample into 10 mL specific working solvent. Then, the solvent with the sample in it was ultrasonicated for a certain time in an ultrasonic cleaner, with a constant power of 100 W. The obtained solution was centrifuged under a speed of 2000 rpm/min one time to remove the working solvent and another time using ethanol to disperse the recycled AgNW in ethanol. It is noted that the second centrifugation process that replaces the dispersion solvent with ethanol is to ensure the same solvent used for the original and recycled NWs when drop-casting, and remove

the potential influence to percolation network properties caused by different solvents. After the centrifugation, 1 mL recycled AgNWs solution in ethanol was stored in a vessel, followed by the drop casting step to fabricate a recycled AgNW network for characterization or the next recycling. All the recycled NWs from one sample (with a loading density of 20 μg/cm^2 on a 2 cm by 2 cm glass slide) are drop-casted onto new glass slides with the same size of 2 cm by 2 cm and dried, to compare the morphology and electrical properties between the original and recycled NW networks. While the area of the drop-casted recycled AgNW network is the same as the original sample, the loading density likely decreases due to the loss during the recycling process. In experiments of using different working solvents to recycle AgNWs, MeOH, EtOH, IPA, EG, and DI water were used during ultrasonication. Recycling by different ultrasonic time, ranging from 5 to 60 s, was studied.

Morphology characterization: The original and recycled AgNW networks were characterized by SEM. The length of AgNWs were measured by processing the SEM images using a Java based image processing software (ImageJ). Over 1,000 individual NWs were measured in each case. The AF of the drop casted network film was calculated by the following formula:

$$AF = \frac{\text{Area covered by AgNWs}}{\text{Area of image}}$$

To make sure the thresholds in each image were consistent, average diameter of NWs was used as the reference parameter for each image. Threshold results with the same average diameter of NWs were applied for the AF analysis. $\overline{AF}$ was obtained by calculating 40 images of different location from each sample and averaging the results. σ_{AF} was calculated from the Gaussian fitted distribution results of 40 images.

Fabrication of sustainable transient sensors: The original or recycled AgNWs dispersed in ethanol were drop casted onto a glass substrate with a laser scribed Kapton mask to define the designed sensor patterns (Peano curve for temperature sensor and interdigitated pattern for hydration sensor). After drying the solvent and removing the mask, 10% wt PVA aqueous solution with 2 M LiCl as the water-retaining agent was spun coated on the AgNW pattern. The PVA was dried at 50 ℃ for 6 hours and then peeled off from the glass substrate. As a result, the AgNW patterns were transferred to the PVA substrate and semi-embedded under the surface of PVA thin film.

Sheet resistance measurement: A typical four probe measurement was carried out to obtain the sheet resistance of each AgNW network film. Three samples of each case were tested and the average sheet resistance was analyzed.

Supplementary Materials

Supporting Information is available from the Wiley Online Library or from the author.

Acknowledgements

The authors gratefully acknowledge the financial support from the National Science Foundation under Award No. CMMI-1728370.

Received: ((will be filled in by the editorial staff))

Revised: ((will be filled in by the editorial staff))

Published online: ((will be filled in by the editorial staff))

References

[1] J. B. Zimmerman, P. T. Anastas, H. C. Erythropel, W. Leitner, *Science* **2020,** *367* (6476), 397-400.

[2] V. R. Feig, H. Tran, Z. Bao, *ACS Cent Sci* **2018,** *4* (3), 337-48.

[3] M. Gao, C.-C. Shih, S.-Y. Pan, C.-C. Chueh, W.-C. Chen, *J. Mater. Chem. A* **2018,** *6* (42), 20546-63.

[4] M. Irimia-Vladu, *Chem. Soc. Rev.* **2014,** *43* (2), 588-610.

[5] J. A. Rogers, T. Someya, Y. Huang, *Science* **2010,** *327* (5973), 1603-7.

[6] T. Sekitani, T. Yokota, U. Zschieschang, H. Klauk, S. Bauer, K. Takeuchi, M. Takamiya, T. Sakurai, T. Someya, *Science* **2009,** *326* (5959), 1516-9.

[7] D. H. Kim, J. H. Ahn, W. M. Choi, H. S. Kim, T. H. Kim, J. Song, Y. Y. Huang, Z. Liu, C. Lu, J. A. Rogers, *Science* **2008,** *320* (5875), 507-11.

[8] D. J. Lipomi, M. Vosgueritchian, B. C. Tee, S. L. Hellstrom, J. A. Lee, C. H. Fox, Z. Bao, *Nat. Nanotechnol.* **2011,** *6* (12), 788-92.

[9] D. Son, J. Lee, S. Qiao, R. Ghaffari, J. Kim, J. E. Lee, C. Song, S. J. Kim, D. J. Lee, S. W. Jun, S. Yang, M. Park, J. Shin, K. Do, M. Lee, K. Kang, C. S. Hwang, N. Lu, T. Hyeon, D. H. Kim, *Nat. Nanotechnol.* **2014,** *9* (5), 397-404.

[10] Z. Zhou, K. Chen, X. Li, S. Zhang, Y. Wu, Y. Zhou, K. Meng, C. Sun, Q. He, W. Fan, E. Fan, Z. Lin, X. Tan, W. Deng, J. Yang, J. Chen, *Nat. Electron.* **2020,** *3* (9), 571-8.

[11] S. Gong, W. Schwalb, Y. Wang, Y. Chen, Y. Tang, J. Si, B. Shirinzadeh, W. Cheng, *Nat. Commun.* **2014,** *5*, 3132, 1-8.

[12] M. Kaltenbrunner, T. Sekitani, J. Reeder, T. Yokota, K. Kuribara, T. Tokuhara, M. Drack, R. Schwodiauer, I. Graz, S. Bauer-Gogonea, S. Bauer, T. Someya, *Nature* **2013,** *499* (7459), 458-63.

[13] S. Yao, P. Swetha, Y. Zhu, *Adv. Healthc. Mater.* **2018,** *7* (1), 1700889.

[14] S. Xu, Z. Yan, K. I. Jang, W. Huang, H. Fu, J. Kim, Z. Wei, M. Flavin, J. McCracken, R. Wang, A. Badea, Y. Liu, D. Xiao, G. Zhou, J. Lee, H. U. Chung, H. Cheng, W. Ren, A. Banks, X. Li, U. Paik, R. G. Nuzzo, Y. Huang, Y. Zhang, J. A. Rogers, *Science* **2015,** *347* (6218), 154-9.

[15] Z. Xue, H. Song, J. A. Rogers, Y. Zhang, Y. Huang, *Adv. Mater.* **2019**, e1902254.

[16] S. W. Hwang, H. Tao, D. H. Kim, H. Cheng, J. K. Song, E. Rill, M. A. Brenckle, B. Panilaitis, S. M. Won, Y. S. Kim, Y. M. Song, K. J. Yu, A. Ameen, R. Li, Y. Su, M. Yang, D. L. Kaplan, M. R. Zakin, M. J. Slepian, Y. Huang, F. G. Omenetto, J. A. Rogers, *Science* **2012,** *337* (6102), 1640-4.

[17] C. J. Bettinger, Z. Bao, *Adv. Mater.* **2010,** *22* (5), 651-5.

[18] S. W. Hwang, G. Park, H. Cheng, J. K. Song, S. K. Kang, L. Yin, J. H. Kim, F. G. Omenetto, Y. Huang, K. M. Lee, J. A. Rogers, *Adv. Mater.* **2014,** *26* (13), 1992-2000.

[19] T. Lei, M. Guan, J. Liu, H. C. Lin, R. Pfattner, L. Shaw, A. F. McGuire, T. C. Huang, L. Shao, K. T. Cheng, J. B. Tok, Z. Bao, *Proc. Natl. Acad. Sci. U.S.A* **2017,** *114* (20), 5107-12.

[20] Z. Zou, C. Zhu, Y. Li, X. Lei, W. Zhang, J. Xiao, *Sci. Adv.* **2018,** *4* (2), eaaq0508.

[21] P. Lee, J. Lee, H. Lee, J. Yeo, S. Hong, K. H. Nam, D. Lee, S. S. Lee, S. H. Ko, *Adv. Mater.* **2012,** *24* (25), 3326-32.

[22] F. Xu, Y. Zhu, *Adv. Mater.* **2012,** *24* (37), 5117-22.

[23] Z. Cui, Y. Han, Q. Huang, J. Dong, Y. Zhu, *Nanoscale* **2018,** *10* (15), 6806-11.

[24] S. Yao, A. Myers, A. Malhotra, F. Lin, A. Bozkurt, J. F. Muth, Y. Zhu, *Adv. Healthc. Mater.* **2017,** *6* (6), 1601159.

[25] M. Amjadi, A. Pichitpajongkit, S. Lee, S. Ryu, I. Park, *ACS Nano* **2014,** *8* (5), 5154-63.

[26] S. Choi, J. Park, W. Hyun, J. Kim, J. Kim, Y. B. Lee, C. Song, H. J. Hwang, J. H. Kim, T. Hyeon, D. H. Kim, *ACS Nano* **2015,** *9* (6), 6626-33.

[27] Z. Cui, F. R. Poblete, Y. Zhu, *ACS Appl. Mater. Interfaces* **2019,** *11* (19), 17836-17842.

[28] S. Liu, S. Ho, F. So, *ACS Appl. Mater. Interfaces* **2016,** *8* (14), 9268-74.

[29] Z. Yu, Q. Zhang, L. Li, Q. Chen, X. Niu, J. Liu, Q. Pei, *Adv. Mater.* **2011,** *23* (5), 664-8.

[30] L. Hu, H. S. Kim, J. Y. Lee, P. Peumans, Y. Cui, *ACS Nano* **2010,** *4* (5), 2955-63.

[31] S. Ye, A. R. Rathmell, Z. Chen, I. E. Stewart, B. J. Wiley, *Adv. Mater.* **2014,** *26* (39), 6670-87.

[32] L. Yang, T. Zhang, H. Zhou, S. C. Price, B. J. Wiley, W. You, *ACS Appl. Mater. Interfaces* **2011,** *3* (10), 4075-84.

[33] M. Park, J. Im, M. Shin, Y. Min, J. Park, H. Cho, S. Park, M. B. Shim, S. Jeon, D. Y. Chung, J. Bae, J. Park, U. Jeong, K. Kim, *Nat. Nanotechnol.* **2012,** *7* (12), 803-9.

[34] Y. Zhu, F. Xu, *Adv. Mater.* **2012,** *24* (8), 1073-7.

[35] H. Jang, Y. J. Park, X. Chen, T. Das, M. S. Kim, J. H. Ahn, *Adv. Mater.* **2016,** *28* (22), 4184-202.

[36] R. M. Fernandes, B. Abreu, B. Claro, M. Buzaglo, O. Regev, I. Furo, E. F. Marques, *Langmuir* **2015,** *31* (40), 10955-65.

[37] Y. G. Sun, Y. N. Xia, *Adv. Mater.* **2002,** *14* (11), 833-7.

[38] S. Y. Chen, Y. W. Guan, Y. Li, X. W. Yan, H. T. Ni, L. Li, *J. Mater. Chem. C* **2017,** *5* (9), 2404-14.

[39] S. E. Skrabalak, B. J. Wiley, M. Kim, E. V. Formo, Y. N. Xia, *Nano letters* **2008,** *8* (7), 2077-81.

[40] G. Hu, J. Kang, L. W. T. Ng, X. Zhu, R. C. T. Howe, C. G. Jones, M. C. Hersam, T. Hasan, *Chem. Soc. Rev.* **2018,** *47* (9), 3265-300.

[41] Y. Y. Huang, T. P. J. Knowles, E. M. Terentjev, *Adv. Mater.* **2009,** *21*, 3945-48.

[42] X. Yu, X. Yu, J. Zhang, L. Chen, Y. Long, D. Zhang, *Nano Res.* **2017,** *10* (11), 3706-14.

[43] S. M. Bergin, Y. H. Chen, A. R. Rathmell, P. Charbonneau, Z. Y. Li, B. J. Wiley, *Nanoscale* **2012,** *4* (6), 1996-2004.

[44] S. Sorel, P. E. Lyons, S. De, J. C. Dickerson, J. N. Coleman, *Nanotechnology* **2012,** *23* (18), 185201.

[45] F. Hennrich, R. Krupke, K. Arnold, J. A. Rojas Stutz, S. Lebedkin, T. Koch, T. Schimmel, M. M. Kappes, *J Phys Chem B* **2007,** *111* (8), 1932-7.

[46] A. Lucas, C. Zakri, M. Maugey, M. Pasquali, P. van der Schoot, P. Poulin, *J. Phys. Chem. C* **2009,** *113* (48), 20599-605.

[47] M. Wan, J. Tao, D. Jia, X. Chu, S. Li, S. Ji, C. Ye, *CrystEngComm* **2018,** *20* (20), 2834-40.

[48] J. Wang, J. Jiu, T. Araki, M. Nogi, T. Sugahara, S. Nagao, H. Koga, P. He, K. Suganuma, *Nanomicro Lett* **2015,** *7* (1), 51-8.

[49] X. Huang, H. Cheng, K. Chen, Y. Zhang, Y. Zhang, Y. Liu, C. Zhu, S. C. Ouyang, G. W. Kong, C. Yu, Y. Huang, J. A. Rogers, *IEEE Trans Biomed Eng* **2013,** *60* (10), 2848-57.

[50] S. Yao, J. Yang, F. R. Poblete, X. Hu, Y. Zhu. *ACS Appl. Mater. Interfaces* **2019**, **11**, 31028-37.

Figures and Tables

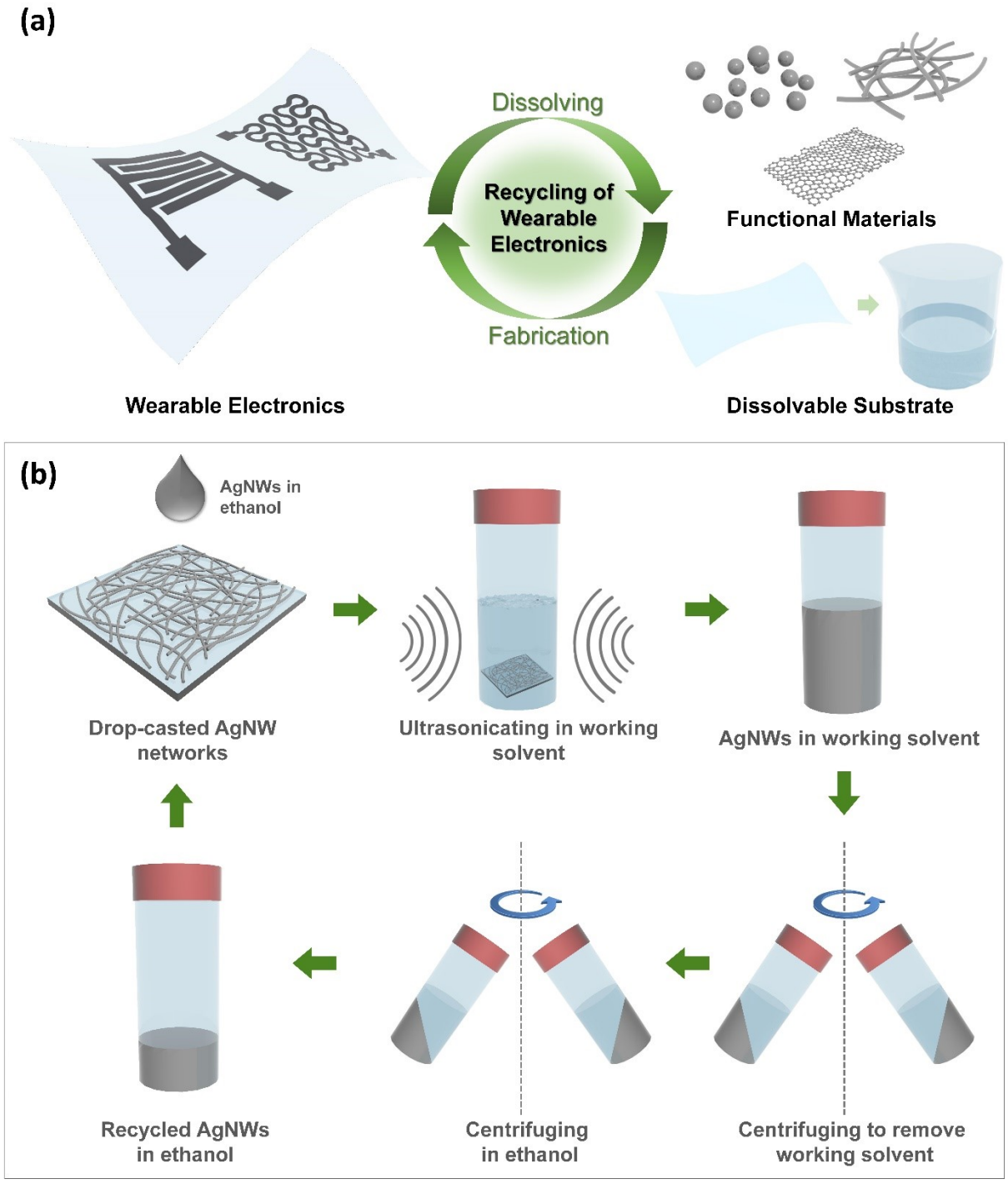

Figure 1 a) Schematic illustration for the concept of recycling wearable electronics based on percolation network of nanomaterials. b) Schematic illustration of the recycling process for drop-casted AgNW percolation network.

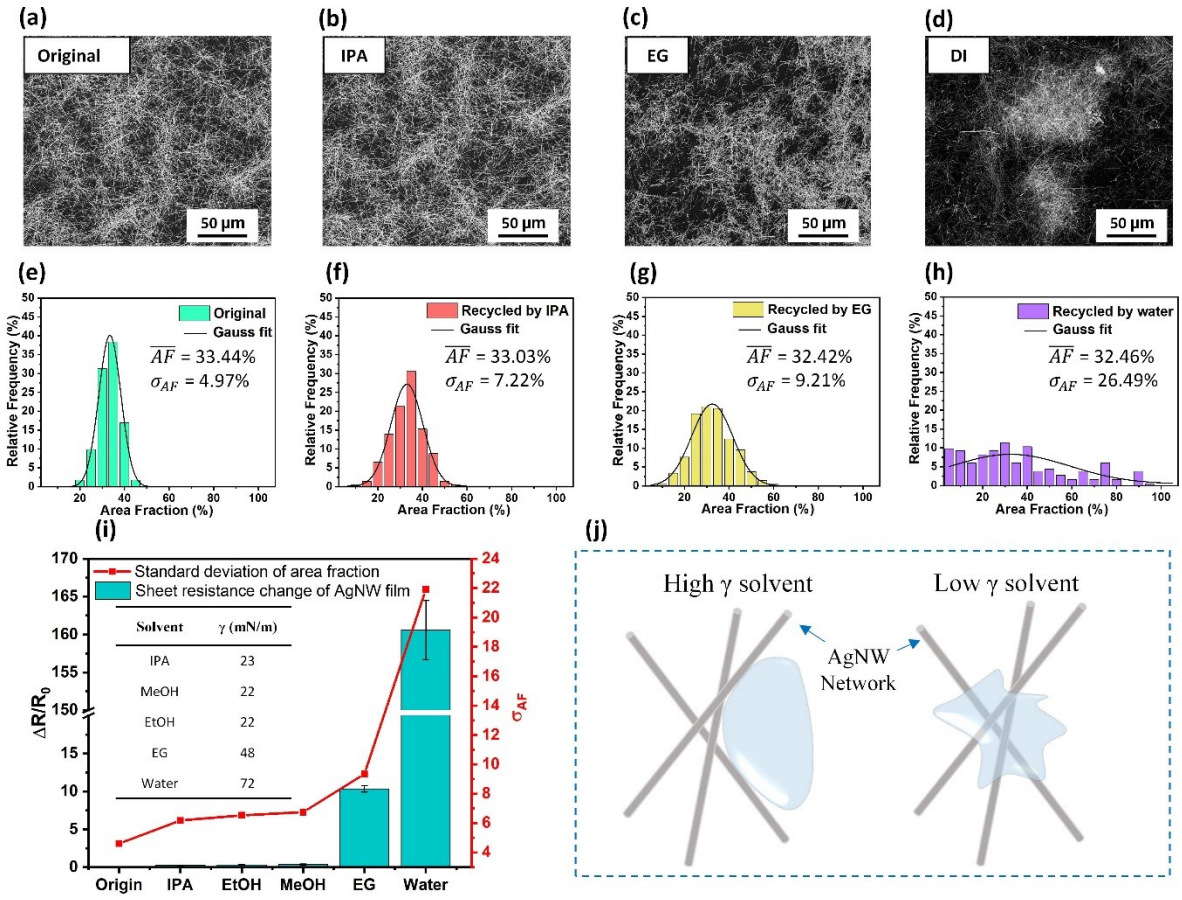

Figure 2 Representative SEM images of a) original AgNW network and recycled AgNW network using b) IPA, c) EG and d) DI water as working solvent. AF distribution and the Gaussian fit results of e) original AgNW network and recycled AgNW network using f) IPA, g) EG and (h) DI water as working solvent. i) The sheet resistance change (left axis) and the standard deviation of AF, σ_{AF} (right axis), of the original AgNW network and recycled AgNW network using IPA, EtOH, MeOH, EG and DI water as working solvents. The inset table shows the surface tension of the working solvents used here. j) Schematic diagrams of wetting AgNW junctions with solvent of different surface tension γ.

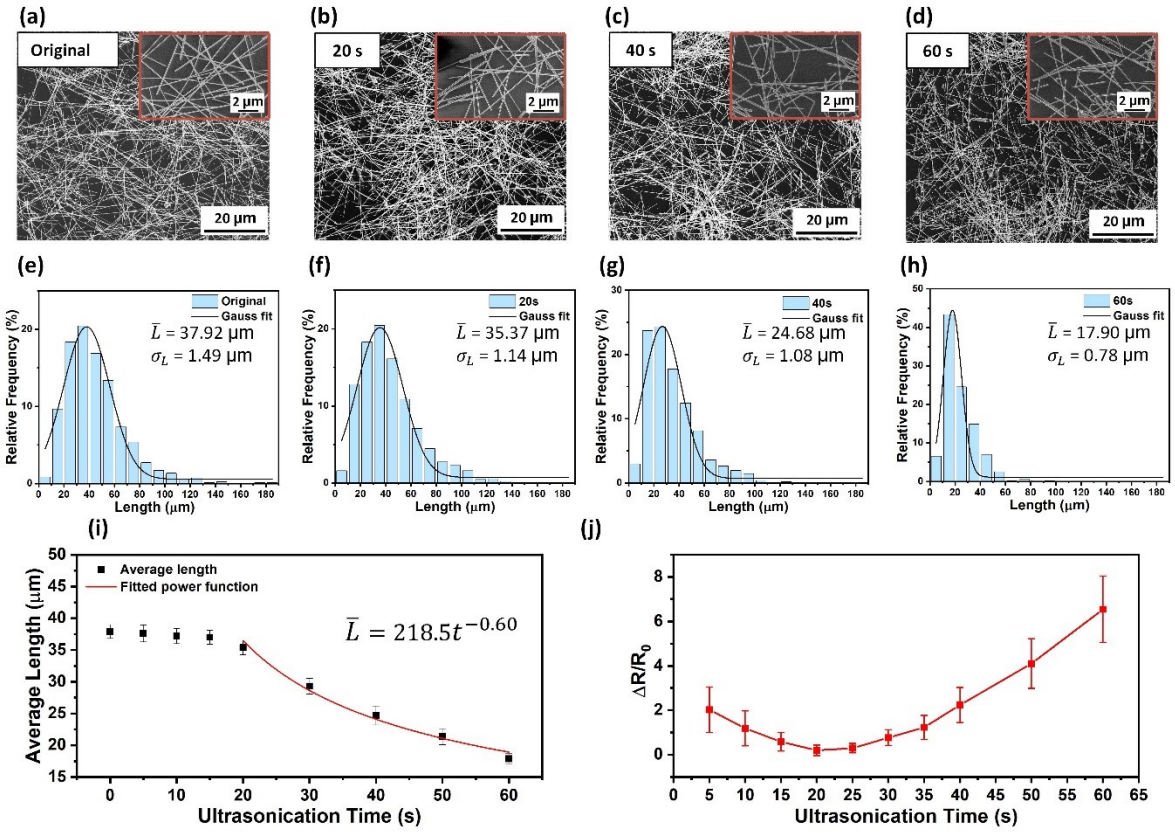

Figure 3 Representative SEM images of a) original AgNW network and recycled AgNW network by ultrasonication time of b) 20 s, c) 40 s and d) 60 s. Scale bar: 10 μm. Length distribution and the Gaussian fit results of e) original AgNW network and recycled AgNW network by ultrasonic time of f) 20 s, g) 40 s and h) 60 s. i) The average length of 1,000 individual NWs recycled by different ultrasonic time (error bars represent the standard deviations) and the power function fit results of the scatters when the ultrasonic time is above 20 s. j) Sheet resistance change of drop-casted AgNW network recycled by different ultrasonic time.

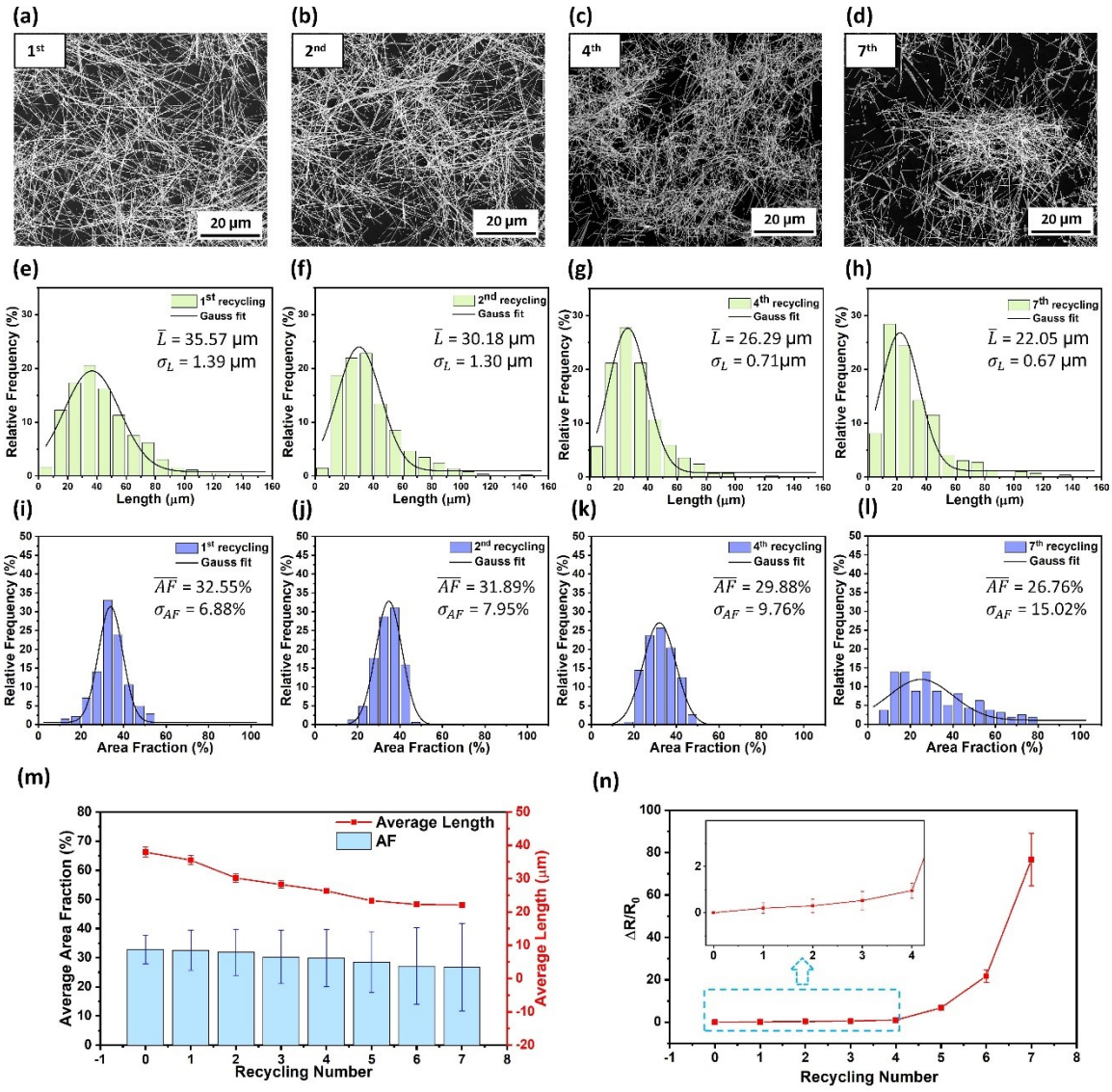

Figure 4 Representative SEM images of recycled AgNW network by different recycling numbers of a) 1st, b) 2nd, c) 4th and d) 7th. Scale bar: 10 μm. Length distribution and the Gaussian fit results of recycled AgNW network by different recycling numbers of e) 1st, f) 2nd, g) 4th, and h) 7th. AF distribution and the Gaussian fit results of recycled AgNW network by different recycling numbers of i) 1st, j) 2nd, k) 4th, and l) 7th. m) $\overline{AF}$ (left axis) of 40 optical images and $\bar{L}$of 1,000 individual NWs (right axis) recycled after different recycling numbers. The error bars represent the standard deviation. n) Sheet resistance change of drop-casted AgNW network recycled after different recycling numbers. Inset is the magnified plot within the first 4th recycling.

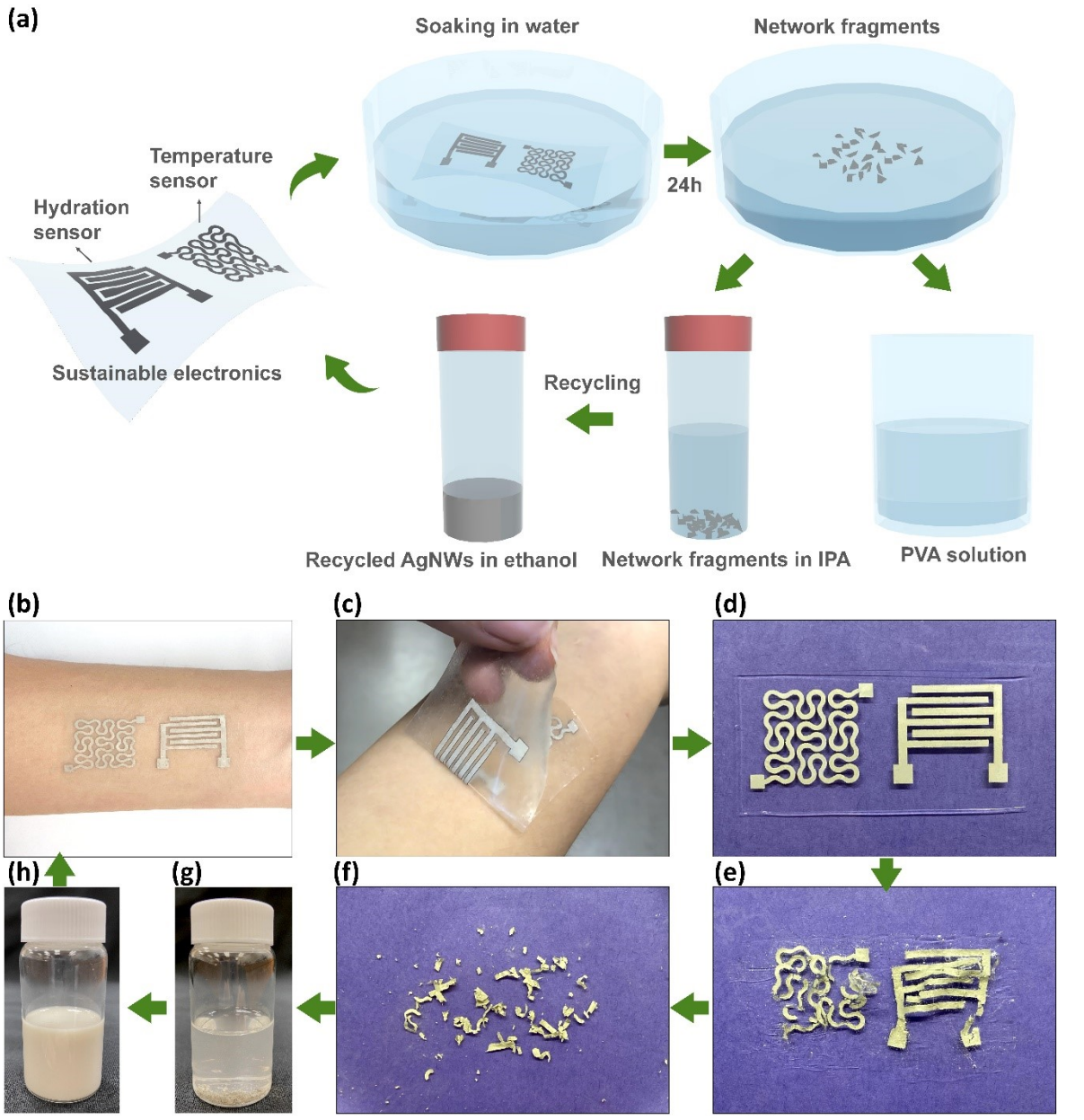

Figure 5 a) Schematic illustration of the recycling process for the sustainable tranient sensor patch. b) Image of the sensor patch worn on the forearm of a human subject. c) Image of the sensor patch being peeled off the skin. Images of the sensor patch when soaked under water d) at beganing , e) after 1 m, and f) after 24 h. g) Image of collected disintegrated AgNW film pieces in IPA h) Image of the recycled AgNWs dispersed in ethanol.

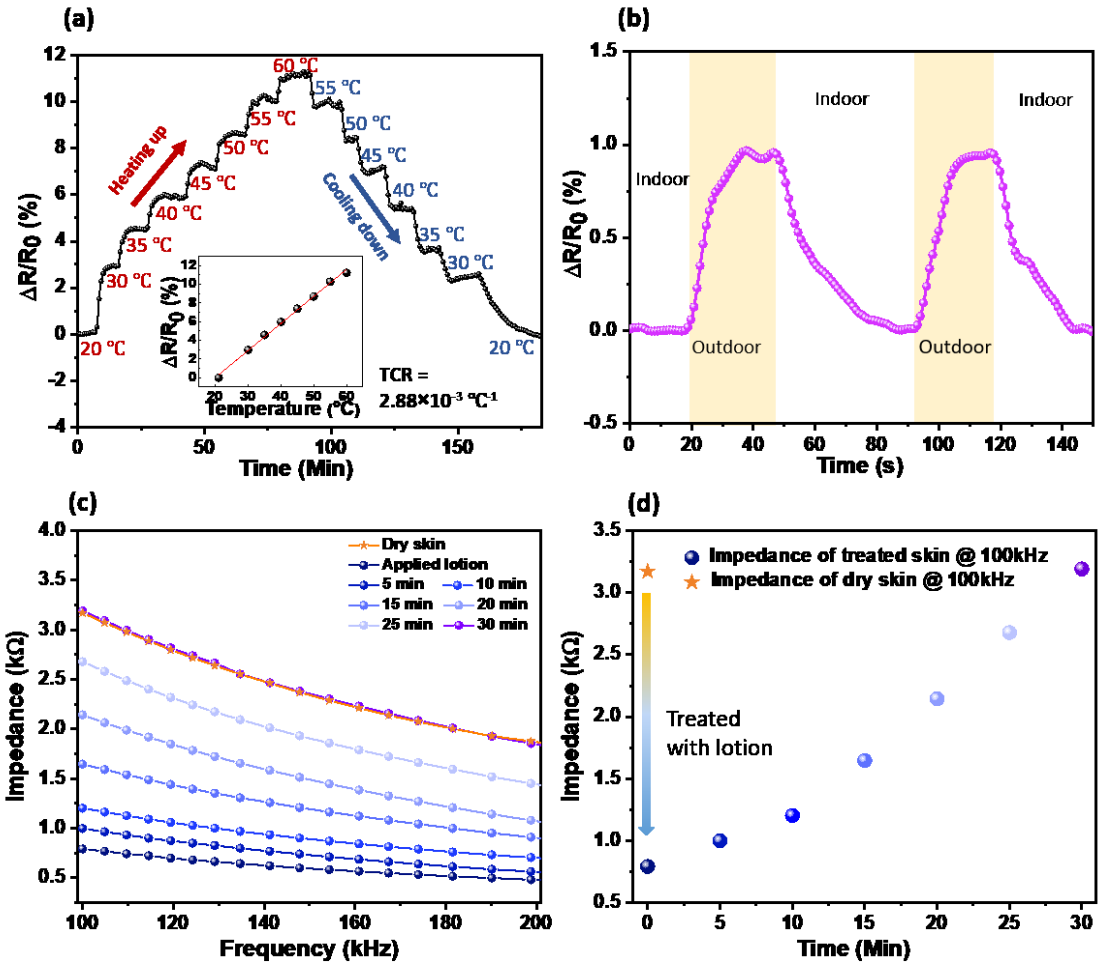

Figure 6 a) Resistance change of the recycled temperature sensor with incremental and degressive temprature change from 20 to 60 °C. Inset shows the resistance change as a function of temperature and the linear fit that gives rise to TCR. b) Real-time measurement data from on-body test of the recycled temperature sensor when the subject went outdoor and back indoor. c) Impedance of the recycled hydration sensor before and after applying lotion on skin. d) Extracted impedance values at 100 kHz before and after applying lotion.